Biol. Cybernetics 34, 63–79 (1979)

Biological Cybernetics

Analysis of "Integrate-to-Threshold" Neural Coding Schemes

A. M. Bruckstein and Y. Y. Zeevi

Faculty of Electrical Engineering, Technion – Israel Institute of Technology, Haifa, Israel

Abstract. Methods of analysis for some deterministic and stochastic variants of the integrate-to-threshold neural coding scheme are presented. Adaptation phenomena are modeled by means of feedforward and feedback adaptive threshold control. Simulations of sinusoidal and step responses reproduce satisfactorily the qualitative characteristics of adaptation as compared with physiological data. It is postulated that such adaptive threshold control may be accomplished by the release, or conformation change, of molecules involved in the control of excitable-channel dynamics.

I. Introduction

It is well established that transmission of information over relatively long distances in the nervous system is accomplished by means of a nonlinear mechanism of excitable membranes, which generates all-or-none stereotyped pulses of depolarization and propagates them along neuronal axons (Hodgkin, 1964; Cole, 1968; Bullock, 1959). Trains of such "spikes" or "action potentials" carry pulse-coded information, for example from peripheral sensory transducers to the central nervous system (along the afferent pathways) and from it to the motor units (along the afferent pathways). It is the function of neural encoders to transform time-varying analog signals, such as sensory transducer's output or other graded potentials resulting from cumulative electrical activity, into sequences of spike discharges. This mode of neural communication raises some important questions concerning the coding process involved at the neuron level and the biologically significant – information-carrying – parameter of the resulting spike trains. Excellent discussions of this topic were presented by several authors (e.g. Perkel and Bullock, 1968; Segundo, 1970; Perkel, 1970; Stein, 1970; Terzuolo, 1970). It is likely that information encoded in spatial patterns of activity utilizing "labeled lines" with built-in connections is more important to the central nervous system than the detailed structure of the time-varying pattern of spike activity on a certain fiber (Perkel and Bullock, 1968). However, study of temporal coding by individual units is relevant, since spatial patterns are generated as a pooling of individual time-varying patterns. Furthermore, certain sensory phenomena are probably coded by the sequence of interspike intervals and not only by the mean rate of firing (Perkel and Bullock, 1968; Chung et al., 1970).

Experimental studies on both the details of action-potential generation at the membrane level and the overall input-output transfer function of the encoder, indicate that:

1. Action-potential discharges occur at a certain threshold level of membrane potential.
2. Up to the firing moment, there is cumulative build-up of sub-threshold membrane depolarization.
3. Changes in the rate of spike occurrence from a certain spontaneous level of activity are proportional to the graded potential input amplitude.
4. Firing of a unit is essentially a probabilistic event, and the interspike intervals are subject to random fluctuation even at constant stimuli.
5. The encoder exhibits saturation as well as adaptive properties, therefore it is a nonlinear time varying, input dependent system.

Extensive experimental work, resulting in a vast volume of data, led to development of several neural encoder models. In spite of obvious over-simplifications, these models permit digital simulation and mathematical analysis, with valuable insight into the coding process (Siebert, 1970; Lee, 1969; Gestri, 1971; Sanderson and Calvert, 1973; Sugiyama et al., 1970; Zeevi and Bruckstein, 1977). For the analysis of such models, concepts and techniques of communi-

0340-1200/79/0034/0063/$03.40

cation and information theory are useful and available. In addition, this approach permits meaningful comparison between the performance of biological and engineering communication systems (Stein, 1970; Stein et al., 1972; Gerstein and Perkel, 1972; Knox, 1970; Walløe, 1968). Both deterministic and stochastic pulse-modulation schemes were considered in the search for an adequate model of the neural encoder.

The probabilistic approach, implied by the existence of fluctuations (Verveen and De Felice, 1974) and necessitated by the difficulties in allowing for the formidable complexity of the process, treats the activity registered on the nerve fiber as essentially random sequences of pulses carrying information in terms of some of the overall statistical parameters, for example the mean rate of occurrence (Siebert, 1970; Gestri, 1971; Bayly, 1968), or the interspike interval distribution (Perkel and Bullock, 1968; Sanderson and Calvert, 1973). Thus rate modulators for a stochastic point process (usually the classic Poisson process) were employed in describing the behavior of the neural encoder. This approach, however, regards the neuron as a black box and does not take into account several essentials of the coding process.

The "Integrate-to-Threshold" (ITT) model, or the "Integral Pulse Frequency Modulation" (IPFM) has several advantages in this context. Indeed, its definition is an adequate mathematical description of what physiologists believe to be the process of spike generation at the membrane level. Furthermore, the behavior of this model corresponds to some of the important experimental fidings and is relatively easy to handle mathematically (Lee, 1969; Gestri, 1971; Zeevi and Bruckstein, 1977; Li, 1961; Bayly, 1968). A further advantage of the above model is its suitability for unified representation of assorted schemes – for example, some of the stochastic black-box models are obtainable through incorporation of random fluctuations in the ITT model.

In this work, we present methods of analysis for some deterministic and stochastic variants of the integrate-to-threshold scheme. The model is then modified to account for adaptation phenomena. Finally, spectral analysis of the spike trains obtained from the models discussed is used in estimating the capability of the neural system to convey information reliably.

II. The Neural Encoder Model

Let $\lambda(t)>0$, denote the time varying intensity of the stimulus applied to the encoder – the input function. In the following analysis we shall consider the input, $\lambda(t)$, to be a deterministic function which is a realization of a continuous stochastic process $\{\Lambda(t)\}$.

The ITT encoder model can be described as follows: integration is performed on the positive input $\lambda(t)$ and an action potential impulse is initiated when the integral representing the cumulated membrane depolarization reaches a certain threshold value. The integrator is then reset and the whole process restarted (Lee, 1969; Gestri, 1971).

At low firing rates, the action potential pulse is of short duration compared to the interspike intervals, and can therefore be modelled as a Dirac impulse defining the moment of its initiation. Moreover, this assumption is further justified by the fact that whenever neural information has to be transmitted over a long distance (compared to the neuronal fiber space constant), it is encoded in interspike intervals, or times of occurrence, and the action potential shape is quite irrelevant. Accordingly, the encoder output in response to an input $\lambda(t)$ can be given by:

$$f(t)=\sum_k \delta(t-t_k), \tag{1a}$$

where the time of occurrence t_k is defined recursively as the solution of the equation

$$\int_{t_{k-1}}^{t} \lambda(\zeta)d\zeta = A(t), \tag{1b}$$

such that no other solution $t'<t_k$ exists. Here $t_0=0$ is an arbitrarily assigned time origin and $A(t)>0$ is the time varying threshold function.

Thus we have for $t=t_k>t_{k-1}$:

$$\int_{t_{k-1}}^{t_k} \lambda(\zeta)d\zeta = A(t_k). \tag{1c}$$

Note that if a train of pulses with shape $p(t)$ is to be generated, where $p(t)$ accounts for the action potential time course, the output will be:

$$f_p(t)=\sum_k p(t-t_k),$$

or equivalently: $f_p(t)=p(t)*f(t)$, where $*$ denotes the convolution operator. In other words, in order to reconstruct in the model the neuronal signal, a pulse shaping filter with impulse response $p(t)$ can be introduced. A schematic representation of such a general idealized neuronal encoder model is presented in Fig. 1.

The main differences between the various more specific ITT models stem from the underlying assumptions with regard to the threshold function, $A(t)$, as follows:

— A constant threshold, $A(t)=A$, defines a deterministic pulse frequency modulator. The resulting model was extensively analyzed in the context of neural encoders (Lee, 1969; Zeevi and Bruckstein, 1977; Li, 1961; Bayly, 1968).

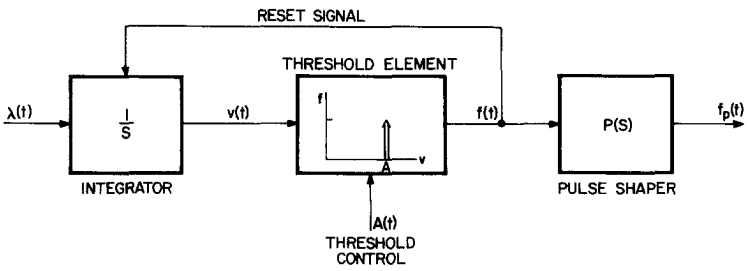

Fig. 1. Schematic block diagram of the general "integrate-to-threshold" encoder. The threshold element indicates that $f(t)=\sum_k \delta(t-t_k)\forall k$ when $v(t_k)=A(t_k)$. $P(s)$ denotes the transfer function of a pulse shaper such as an action potential generator

— If one assumes that the threshold $A(t)=A_k$ is constant only over the interspike interval (t_{k-1}, t_k), the A_k's being random, a stochastic model with some very interesting properties is obtained (Gestri, 1971).

— When $A(t)$ is considered to change in a certain adaptive way, a complicated output feedback or input feedforward scheme is obtained.

— Finally, if $A(t)$ is taken as a continuous random function, determination of the encoder output reduces to a classical crossing problem. This has not yet been analytically solved, and encoder behaviour is usually simulated on a digital or an analog computer.

Another possible modification of the integrate-to-threshold model is weighted integration of the input at the membrane level, accounting for the leaky properties (the leaky SSIPFM model) (Poppele and Chen, 1972).

III. The Deterministic IPFM and its Equivalence to Other Pulse Modulation Schemes

In the case of constant encoder threshold $A(t)=A>0$, and positive input $\lambda(t)$, the model is called Single Signed Integral Pulse Frequency Modulation (SS-IPFM). Extensive theoretical work on this model was reported by Li (1961), Lee (1969), and Bayly (1968). Lee introduced a "functional model" for the encoder useful in spectral analysis and also established that SS-IPFM is identical to Continuous Pulse Frequency Modulation. This result and the proof of equivalence between SS-IPFM and the naturally sampled Pulse Position Modulation (PPM) are readily obtained directly from the definition of these modulation schemes (Zeevi and Bruckstein, 1977; Rowe, 1965; Carlson, 1975).

A) From the definition of the generalized encoder (1), setting $A(t)=A$, we have for the SS-IPFM output:

$$f_{\text{SSIPFM}}(t)=\sum_k \delta(t-t_k), \tag{2a}$$

where the times of occurrence of consecutive impulses are related by:

$$\int_{t_{k-1}}^{t_k} \lambda(\zeta)d\zeta = A. \tag{2b}$$

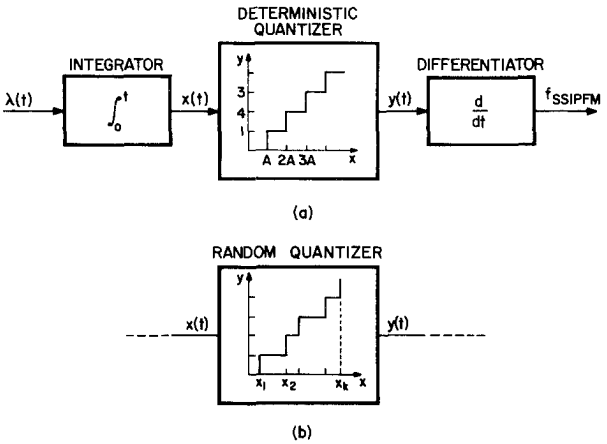

Fig. 2a and b. Functional model of a deterministic **a** and random **b** SSIPFM encoder (modified from [19]). The deterministic quantizer has the input-output function: $y=\mathscr{F}(x)=k$ if $x\in(x_k, x_{k+1})$, $x_0=0$ and $x_k=kA$. The random-jump-point quantizer has an input-output function: $y=\mathscr{F}_r(x)=k$ if $x\in(x_k, k_{k+1})$, $x_0=0$ and the random variable $x_k=\sum_1^{k-1} A_k$

It is easily seen that, provided $t_0=0$ is the time origin as before, an equivalent expression for (2b), defining t_k implicitly but *not* recursively, is:

$$\int_0^{t_k} \lambda(\zeta)d\zeta = kA. \tag{2c}$$

It can be easily checked that the "functional model", given in Fig. 2, generates the encoder output defined above. As already emphasized by Lee, this scheme is useful for the analysis but clearly cannot be directly implemented since both integrator and quantizer must have infinite dynamic range.

B) Let us now consider the Continuous Pulse Freqency Modulation (CPFM) defined as a train of spikes occurring at the zero crossings of a Frequency Modulated (FM) sinusoidal continuous wave:

$$f_{\text{CPFM}}(t)=\sum_k \delta(t-t_k), \tag{3a}$$

where t_k's are the zero crossings of the FM wave defined for convenience as:

$$f_{\text{FM}}(t)=K\cdot\sin\left[\frac{\pi}{A}\int_0^t \lambda(\zeta)d\zeta\right],$$

and $\lambda(t)$ is the modulating input function.

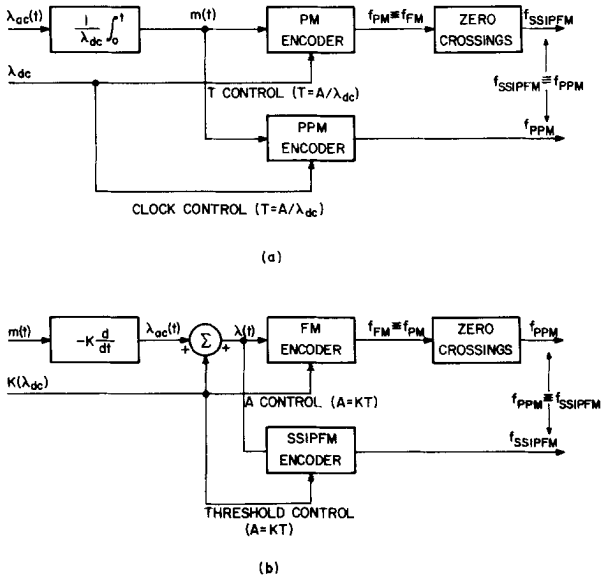

Fig. 3a and b. Diagrams illustrating the relationships between the various modulation schemes. **a** SSIPFM encoded signal obtained by means of a PM encoder and its PPM equivalent. **b** PPM encoded signal obtained by means of an FM encoder and its SSIPFM equivalent

Using the above definition of FM, we have the following expression for the k-th zero crossing:

$$\frac{\pi}{A}\int_0^t \lambda(\zeta)d\zeta = k\pi$$

or

$$\int_0^t \lambda(\zeta)d\zeta = kA$$

which is identical to (2c).

Note that the FM wave is usually defined in communication textbooks (Rowe, 1965; Carlson, 1975) as:

$$f_{\mathrm{FM}} = K\sin\left[\omega_c t + 2\pi f_\Delta \int_0^t s(\zeta)d\zeta\right]$$

where ω_c is the carrier frequency, $s(\cdot)$ the a.c. modulating function, and f_Δ the frequency deviation constant.

Thus, *identical pulse trains* are defined by the SS-IPFM and CPFM encoders if the corresponding FM wave has a carrier frequency of

$$\omega_c = 2\pi\frac{\lambda_{\mathrm{dc}}}{2A},$$

an a.c. modulating function $s(t)=\lambda_{\mathrm{ac}}(t)$, and a frequency derivation constant $f_\Delta = \dfrac{1}{2A}$.

This result, derived first by Lee (1969), makes it possible to apply results readily available from communication theory to the study of neural encoders. The same rationale motivates the search for similarities to other pulse modulation techniques.

C) The Naturally Sampled Pulse Position Modulation is defined as:

$$f_{\mathrm{PPM}}(t) = \sum_k \delta(t - t_k) \tag{4a}$$

with t_k's satisfying the equations

$$t - kT = m(t), \quad k \in N, \tag{4b}$$

where $m(t)$ is the a.c. modulating function, with $\dfrac{dm}{dt} < 1$, and T is the clock period.

Modifying the form of (4b), we obtain

$$\int_0^{t_k}\left[1 - \frac{d}{d\zeta}m(\zeta)\right]d\zeta = kT. \tag{4c}$$

Comparing (2c) and (4c), it is apparent that if the SS-IPFM input, $\lambda(t)$, is:

$$\lambda(t) = \frac{A}{T}\left[1 - \frac{d}{dt}m(t)\right], \tag{5a}$$

identical times of occurrence characterize the PPM and the SS-IPFM output functions. This result will be reestablished later, using a PPM spectral analysis technique for the SSIPFM output (Zeevi and Bruckstein, 1977).

Note that (5a) also yields $\lambda_{\mathrm{dc}} = \dfrac{A}{T}$, and

$$m(t) = -\frac{1}{\lambda_{\mathrm{dc}}}\int_0^t \lambda_{\mathrm{ac}}(\zeta)d\zeta. \tag{5b}$$

D) To complete the comparison of pulse modulation schemes, we note that the PPM wave is in fact a "continuous pulse phase modulation" (CPPM) in the sense that its output pulses define exactly the zero crossings of the Phase Modulated (PM) continuous sinusoidal wave. If, for convenience, the PM wave is written as:

$$f_{\mathrm{PM}} = K\sin\left\{2\pi\frac{1}{2T}[t - m(t)]\right\}, \tag{6a}$$

then the equation for the k's zero crossing becomes:

$$2\pi\cdot\frac{1}{2T}[t - m(t)] = k\pi, \tag{6b}$$

and from (6b) we obtain: $t_k - kT = m(t_k)$, which is exactly (4b).

Note that the PM wave given in (6a) has a carrier frequency of $\omega_c = 2\pi\cdot\dfrac{1}{2T}$ and the modulating function is proportional to $m(t)$ (Rowe, 1965; Carlson, 1975).

The above results on the equivalence between different pulse modulation schemes are summarized in Fig. 3.

IV. The Random Threshold Model

Up to this point the threshold, A, was assumed to be a noise-free, constant parameter, characteristic of the encoder. We shall now consider the case in which after emission time t_{k-1}, the threshold assumes a value that is a realization of a random variable, A_k. Let us further assume that the probability density function, $p_{A_k}(a)$, is given for each k, and $p_{A_k}(a)=0$ for $a<0$. [Obviously the SSIPFM model is obtained taking the particular case of $p_{A_k}(a)\to\delta(a-A)$, for all k.] This model was considered by Gestri (1971) who pointed out that, as a direct result of the theory of random point processes, a "good stochastic pulse frequency modulator" is obtained.

Considering again the "functional encoder" of Fig. 2, and accounting for the above modifications, we obtain a quantizer with random jump points (on the input, x, axis) with interval statistics determined by the r.v.'s A_k, $k\in N$. Starting from $x_0=0$ (origin), the jump points are the r.v.'s given by:

$$x_k=\sum_{i=0}^{k-1} A_i, \qquad k\in N. \tag{7}$$

Thus a random point process on the x-axis is constructed, a realization of which defines the quantizer input-output function. This stochastic quantizer is illustrated in Fig. 2b.

The main problem concerning this random model is whether the input function $\lambda(t)$, is properly encoded so that it can be recovered from the output. Obviously, the latter is a random point process in time, with the sequence of occurrences, $\{t_k\}$ defining the instants at which $x(t)=\int_0^t \lambda(\zeta)d\zeta$ is equal to the x_k's -- the jump points of the quantizer. The situation can be illustrated as follows: a traveller on the x-axis with unknown time-varying speed ($\lambda(t)$) sends a radio signal when meeting randomly spread signs (at x_k's) on his way. Knowing the statistics of the distances between consecutive signs on the way, the problem is to find the instantaneous velocity of the traveller from the sequence of signals received from him.

Given the definition of x_k, Eq. (7), and the interval density distributions, $p_{A_k}(a)$, joint probability density functions for the quantizer jump points can be computed over any interval (x_a, x_b). This provides a complete analytical description of the static point process generated on the x-axis. Using the relation between x and the time varying input ("distance vs. velocity") the output point process statistics can be obtained.

A) Let us now find the relation between the *rates* of the output process $\{t_k\}$ and the jump point process $\{x_k\}$.

The x-rate of the process $\{x_k\}$ is defined as:

$$\begin{aligned}\varrho_x(x)&\triangleq E\left\{\frac{\Delta Y}{\Delta x}\right\}\\&=E\left\{\frac{\text{number of jump points in } (x,x+\Delta x)}{\Delta x}\right\}\\&=E\left\{\frac{N_x(x,x+\Delta x)}{x}\right\},\end{aligned} \tag{8}$$

where:

Δx is an interval too short for significant rate changes to occur, but sufficiently long compared to the intervals between successive jump points, and

$E\{\cdot\}$ denotes the ensemble average operator.

The time rate of the output process $\{t_k\}$ is defined as:

$$\begin{aligned}\varrho_{\text{UOT}}(t)&\triangleq E\left\{\frac{\Delta Y}{\Delta t}\right\}\\&=E\left\{\frac{\text{number of occurrences in } (t,t+\Delta t)}{\Delta t}\right\}\\&=E\left\{\frac{N_T(t,t+\Delta t)}{\Delta t}\right\},\end{aligned} \tag{9}$$

where:

Δt is, again, an interval too short for significant rate changes to occur, but long enough compared to interspike intervals.

Now, since $x(t)=\int_0^t \lambda(\zeta)d\zeta$, we can write:

$$\varrho_{\text{OUT}}(t)=E\left\{\frac{N_T(t,t+\Delta t)}{\Delta t}\right\}=E\left\{\frac{N_x[x(t),x(t+\Delta t)]}{\Delta t}\right\}$$

$$=E\left\{\frac{N_x[x(t),x(t+\Delta t)]}{\Delta x}\cdot\frac{x(t+\Delta t)-x(t)}{\Delta t}\right\},$$

and because:

$$\frac{x(t+\Delta t)-x(t)}{\Delta t}\simeq\frac{d}{dt}x(t)=\lambda(t),$$

is a deterministic value, we immediately have:

$$\varrho_{\text{OUT}}(t)=\lambda(t)\cdot E\left\{\frac{N_x[x(t),x(t+\Delta t)]}{\Delta x}\right\}$$

or

$$\varrho_{\text{OUT}}(t)=\lambda(t)\cdot\varrho_x(x(t)). \tag{10}$$

Thus if the "rate" of the $\{x_k\}$ process is a constant, $\varrho_x(x)=\varrho_0$, we have for the output rate

$$\varrho_{\text{OUT}}(t)=\varrho_0\cdot\lambda(t). \tag{10a}$$

Therefore the output rate follows the time varying input function. This result of Gestri (1971) leads to the

conclusion that the model described is in fact a stochastic pulse frequency modulator. Furthermore, since no specific assumptions were made on the threshold random variables, A_k, describing the jump-point interval statistics, result (10) is *generally true.* [In the deterministic case of SSIPFM, we obviously have that $\varrho_0 = 1/A$ is a constant, and thus: $\varrho_{\text{OUT}}(t) = \frac{1}{A} \cdot \lambda(t)$, the meaning of rate in this case being the inverse of the interspike interval.]

B) It is also of interest to compute the probability $P_x[N(x_a, x_b)]$ of exactly N jump points of the $\{x_k\}$ process over the interval (x_a, x_b).

With $P_x[N(x_a, x_b)]$ and the input function $\lambda(t)$ known, the corresponding probability $P_T[N(t_a, t_b)]$ of N occurrences (emitted pulses) at the encoder output during the interval (t_a, t_b) is readily obtained, since:

$$P_T[N(t_a, t_b)] = P_x[N(x(t_a), x(t_b))],$$

and this yields immediately

$$P_T[N(t_a, t_b)] = P_x\left[N\left(\int_0^{t_a} \lambda(\zeta)d\zeta, \int_0^{t_b} \lambda(\zeta)d\zeta\right)\right]. \tag{11}$$

Let us now assume that the random variables A_k, defining the process $\{x_k\}$ in (7) are statistically independent and that the probability density functions, $p_{A_k}(a)$, are known for each k. It is a classical result that if:

$$p_{A_k}(a) = \varrho_0 e^{-\varrho_0 a} U(a) \quad \text{for each } k,$$

[$U(a)$ denoting the unit step function], then the process $\{x_k\}$ defined in (7) is a Poisson-process with mean ϱ_0 (Gestri, 1971; Papoulis, 1965; Snyder, 1975).

Therefore we have:

$$P_x[N(x_a, x_b)] = [\varrho_0(x_b - x_a)]^N \cdot \exp[-\varrho_0(x_b - x_a)] \cdot (1/N!),$$

and using (11) we obtain for the encoder's output statistics:

$$P_T[N(t_a, t_b)] = \left[\varrho_0 \int_{t_a}^{t_b} \lambda(\zeta)d\zeta\right]^N \cdot \exp\left[-\varrho_0 \int_{t_a}^{t_b} \lambda(\zeta)d\zeta\right] \cdot (1/N!).$$

This is indeed the statistics of a non-uniform Poisson-process with a rate of $\varrho_{\text{OUT}} = \varrho_0 \cdot \lambda(t)$, as expected from the result (10a) of the previous analysis.

Note: if instead of a constant mean ϱ_0, the process $\{x_k\}$ has a non-uniform rate of $\varrho_x(x)$, $P_x[N(x_a, x_b)]$ will be a function of:

$$\int_{x_a}^{x_b} \varrho_x(\zeta)d\zeta \quad \text{instead of } \varrho_0(x_b - x_a) \text{ (Papoulis, 1965).}$$

In this case $P_T[N(t_a, t_b)]$ will be a function of:

$$\int_{\int_0^{t_a} \lambda(\zeta)d\zeta}^{\int_0^{t_b} \lambda(\zeta)d\zeta} \varrho_x(s)ds \quad \text{or} \quad \int_{t_a}^{t_b} \varrho_x\left(\int_0^t \lambda(\zeta)d\zeta\right) \cdot \lambda(t) \cdot dt,$$

and the output rate is therefore

$$\varrho_{\text{OUT}}(t) = \varrho_x(x(t)) \cdot \lambda(t),$$

as expected from the more general result (10).

In conclusion, the Poisson-process rate modulator model is obtained as a particular case of the random integrate-to-threshold model, with an exponential distribution taken for the firing threshold. The distribution assumed is, however, unphysiological.

Experiments performed to test fluctuation phenomena at the neural membrane level (Verveen and De Felice, 1974; Verveen and Derksen, 1968) provide that the relation between probability of response (emission of output pulse) and stimulus intensity applied for a certain fixed duration Δt obeys a Gaussian (erf-shaped) distribution law for independent trials. Furthermore, the mean of the intensity distribution and the standard deviation follow an approximately hyperbolic relation to stimulus duration.

In the context of the random integrate-to-threshold model, the probability of response (action potential emission) to a stimulus of constant intensity, I, applied during a period Δt is:

$$\text{Prob}\left\{\int_0^{\Delta t} \text{Id}\zeta \geqq A_k\right\} = \text{Prob}\{I \cdot \Delta t \geqq A_k\}.$$

Let us assume that the threshold random variables, $\{A_k\}$ have the same distribution for all k, thus the values of the threshold are in fact results of repeated, independent trials on the random variable A with distribution $p_A(a)$.

With $p_A(a)$ known, we can write that

$$\text{Prob}\{I \cdot \Delta t \geqq A\} = \int_0^{I \cdot \Delta t} p_A(a)da. \tag{12}$$

For a constant stimulus duration, $\Delta t = \text{const}$, $\text{Prob}\{I \cdot \Delta t \geqq A\}$ is a function of I only thus, measurement of the probability of response for a range of intensities yields the exact shape of the distribution function for the random variable A. Note that the definition of the distribution function of the r.v. A is $F_A(a) = \text{Prob}\{A < a\}$. Thus we have (Papoulis, 1965) $\text{Prob}\{I \cdot \Delta t > A\} \equiv F_A(I \cdot \Delta t)$. The experimental results provide as stated before a Gaussian (erf shaped) distribution, thus the density is $p_A(a) = \mathcal{N}(A_0, \sigma)$, a classical normal distribution.

[*Note:* since A takes only positive values, a problem seems to arise; but this is not too serious since $p_A(a)$ is narrow around a positive average value and for negative a's the density becomes practically zero.]

The mean of the intensity distribution for a certain Δt is defined as the intensity at which the probability of response is 1/2, thus

$$\text{Prob}\{I_{\text{mean}} \cdot \Delta t \geqq A\} = \tfrac{1}{2}$$

and obviously

$$I_{\text{mean}} \cdot \Delta t = E[A] = A_0 = \text{constant}.$$

Therefore we have $I_{\text{mean}} = \dfrac{A_0}{\Delta t}$, and this explains the hyperbolic relation between mean of the intensity distribution and the stimulus duration, the same being true for the relation between the standard deviation to stimulus duration.

V. Modeling of Adaptation Phenomena

Adaptation is an important functional characteristic encountered at all levels of the organizational hierarchy of the nervous system. Certain adaptive properties are already exhibited by the neuronal encoder at the membrane level. As a result, a positive step change in the encoder input elicits an immediate increase in the rate of firing, followed by a decrease to a certain steady state level of activity. This transient response is attributable in part to adaptation of the neuronal membrane to the new input conditions. In the integrate-to-threshold model there are, basically, two possibilities of accounting for this adaptation phenomenon: (1) interposition of a preprocessing block (Fig. 4a) between the model input and the integrate-to-threshold encoder (Gestri, 1971), and (2) postulation of suitable dynamic behavior for the threshold of the encoder model.

The first approach is rather oversimplified, and provides no insight into the inner mechanisms of the coding process. The preprocessing block is assumed to have a step response similiar to firing rate transients such as observed experimentally in the case of retinal transient x-cells (Enroth-Cugell and Robson, 1966; Wright and Ikeda, 1974).

The level of firing activity affects membrane excitability and the initial local depolarization; this can be modeled through output-rate dependent changes in threshold level. Possible effects of the input on the firing threshold can also be investigated. Let us analyze now some possible adaptation models for the deterministic and stochastic models.

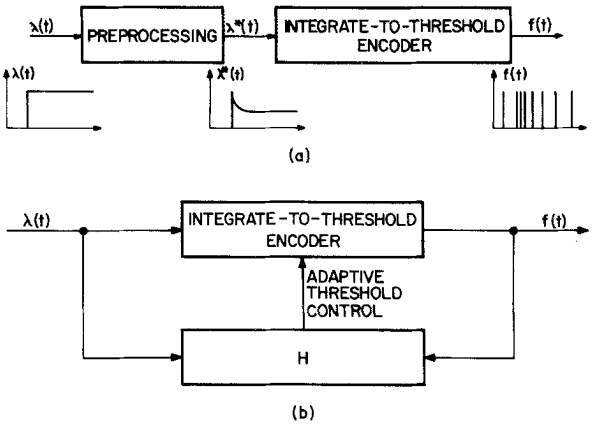

Fig. 4a and b. Modeling adaptation effects by preprocessing of the input $\lambda(t)$ **a**, and by means of adaptive threshold control **b**. $\mathscr{H}$ is a threshold control function operating on both input, $\lambda(t)$, (feedforward) and output, $f(t)$, (feedback). The integrate-to-threshold encoder can be either deterministic or random

A. The Deterministic Case

Consider that instead of being constant, the threshold of the SSIPFM encoder is given by:

$$A(t) = A_0 + A_{\text{ad}}(t) \tag{14}$$

where A_0 is a positive constant, and A_{ad} is the *adaptive* component which is a function of the output rate of occurrence (feedback effect) and of the input level $\lambda(t)$ (feedforward effect). As shown schematically in Fig. 4b, this can be written formally as

$$A_{\text{ad}}(t) = \mathscr{H}(\lambda(t), f(t)),$$

where $\mathscr{H}$ denotes a general threshold control operator.

If the input, $\lambda(t)$, and the threshold, $A(t)$, are slowly changing time functions, the output instantaneous rate, $\varrho_{\text{out}}(t)$, is approximately given by:

$$\varrho_{\text{out}}(t) \simeq \frac{\lambda(t)}{A(t)} = \frac{\lambda(t)}{A_0 + A_{\text{ad}}(t)}. \tag{15}$$

From (15) it is obvious that given a slow dynamic of $A_{\text{ad}}(t)$, a step change in $\lambda(t)$ will result in an immediate change in $\varrho_{\text{out}}(t)$, followed by a transient toward a new steady state determined by the adaptive threshold dynamics.

Three cases of adaptive threshold control can be considered:

1. feedback only – $A_{\text{ad}}(t) = \mathscr{H}_1(\varrho_{\text{out}})$;
2. feedforward only – $A_{\text{ad}}(t) = \mathscr{H}_2(\lambda)$;
3. both feedback and feedforward – $A_{\text{ad}}(t) = \mathscr{H}_1(\varrho_{\text{out}}) + \mathscr{H}_2(\lambda)$,

where the threshold control function, $\mathscr{H}$, has been separated into two distinct (feedback and feedforward) operators $\mathscr{H}_1$ and $\mathscr{H}_2$ respectively.

Assigning to operators $\mathscr{H}_1$ and $\mathscr{H}_2$ d.c. gains of M and N respectively, we can obtain the steady-state output rate of firing for a constant input, λ_0.

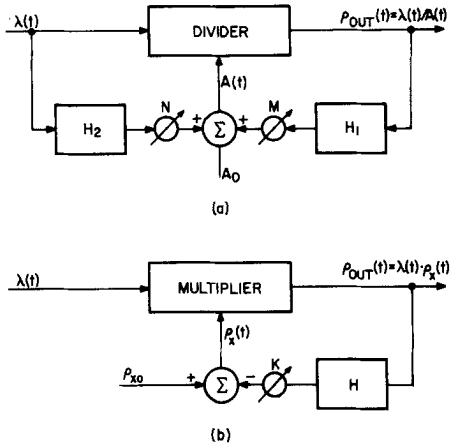

Fig. 5a and b. Models implemented in digital simulation of adaptive effects. **a** The deterministic model using linear first order feedforward and feedback operators. M and N denote variable gains. **b** Simulation of a random threshold model using a deterministic feedback scheme accounting for the mean rate of firing only

In the case of feedback only, we have:

$$\varrho_{\text{out}_{ss}} = \frac{\lambda_0}{A_0 + M\varrho_{\text{out}_{ss}}}$$

yielding:

$$\varrho_{\text{out}_{ss}} = \frac{\sqrt{4M\lambda_0 + A_0^2} - A_0}{2M}.$$

The feedforward case has for the steady state:

$$\varrho_{\text{out}_{ss}} = \frac{\lambda_0}{A_0 + N\lambda_0}.$$

which indicates saturation at high constant input levels ($\varrho_{\text{out}_{ss}} \to 1/N$ as $\lambda_0 \to \infty$).

In the case of both feedback and feedforward we have:

$$\varrho_{\text{out}_{ss}} = \frac{\lambda_0}{A_0 + M\varrho_{\text{out}_{ss}} + N\lambda_0}$$

and the steady state is

$$\varrho_{\text{out}_{ss}} = \frac{\sqrt{N^2\lambda_0^2 + \lambda_0(4M + 2NA_0) + A_0^2} - (N\lambda_0 + A_0)}{2M}.$$

Here again the input-output steady-state function indicates saturation at $\varrho_{\text{outss}} = 1/N$.

Note that *existence* of a steady state is by no means a necessary characteristic feature of a nonlinear control system; the above solutions are correct since a steady state is actually reached.

Further insight into the behavior of the adaptive encoder is obtainable by means of digital simulations. For this purpose we use the approximation given in (15) and the scheme with distinct feedback and feedforward operators for adaptive threshold control. We assume, for the sake of simplicity, that $\mathscr{H}_1$ and $\mathscr{H}_2$ are linear, first-order low pass filters, with d.c. gain 1, cascaded by variable gain controls M and N representing the feedback and feedforward gains respectively, as shown in Fig. 5a. This model was digitally simulated using the CSMP language.

Examples of output instantaneous rate of firing as a function of time are shown for step and sinewave inputs in Figs. 6 and 7 respectively. By choosing the gain parameters M and N, different weights are assigned to feedback and feedforward in the threshold control function. The parametric set of step responses in Fig. 6 exhibit satisfactory adaptation, namely: a sudden increase in the rate of firing at the onset of the step stimulus, decreasing rapidly to a well-defined steady state. These simulated responses confirm the existence of a steady-state as calculated above.

Since sine-waves are used extensively for analysis of cellular input-output functions even where it is known that the system is nonlinear, the adaptive model responses to sinusoidal inputs were determined as well. This permits comparison with experimental results and yields a qualitative idea of distortions caused by adaptive threshold control (see Fig. 7).

One can also attempt to describe these responses analytically by solving the system's differential equations; denoting the feedback and feedforward operators' outputs by $A_1(t)$ and $A_2(t)$ respectively, we have:

$$\begin{cases} \varrho_{\text{out}}(t) = \lambda(t)/(A_0 + MA_1(t) + NA_2(t)) \\ \tau_1 \dfrac{d}{dt} A_1(t) + A_1(t) = \varrho_{\text{out}}(t) \\ \tau_2 \dfrac{d}{dt} A_2(t) + A_2(t) = \lambda(t) \end{cases} \tag{16}$$

where τ_1 and τ_2 are the LPF's time constants.

However, a closed form solution appears to be possible only in a limited number of cases in which it is also quite troublesome to obtain and provides no further insight into the system behavior in the transient phase.

B. The Random Encoder

The random integrate-to-threshold model presented in Sect. IV entails no specific assumptions regarding the threshold random variables A_k. In the most general approach to the adaptation problem, we could assume that the output rate has some effect on the distribution of the threshold random variable. For example, a high rate of activity over a certain time interval would shift the expected value of the random threshold to a higher value and increase the next interspike interval, thereby

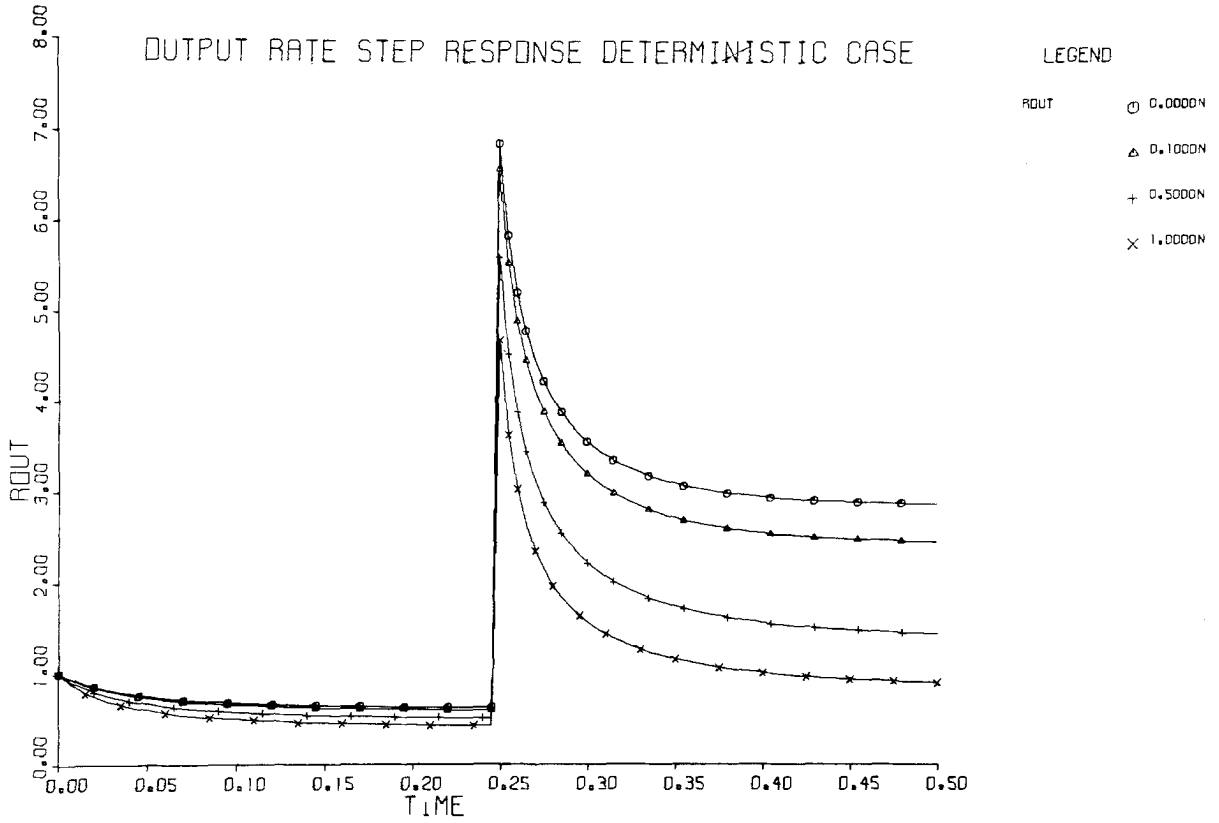

Fig. 6. Parametric set of output rate step responses of the deterministic adaptation model (Fig. 5a). Constant parameters are the feedback gain $M=1.0$, the feedback time constants $\tau_1=\tau_2=0.1$, the step input amplitude $H=10$. The running parameter was the feedforward gain $N=0.0$, 0.1, 0.5, 1.0. Note the system's onset transients for $t \ll 0.25$

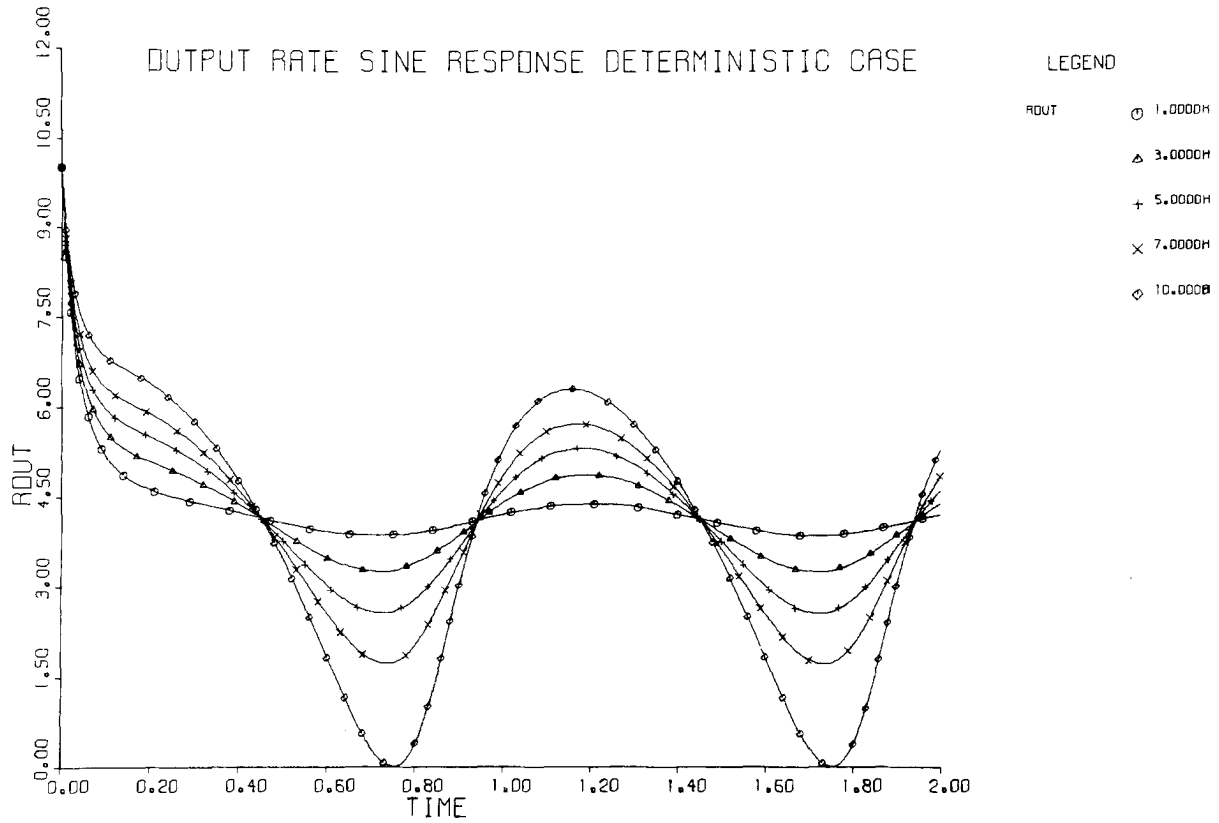

Fig. 7. Output rate sine responses of deterministic model (Fig. 5a) for a range of modulation depth specified by the input amplitudes $H=1.0$, 3.0, 5.0, 7.0, 10, given $M=N=0.1$ and time constants $\tau_1=\tau_2=0.1$. [Input was $\lambda(t)=10+H\cdot\sin 2\pi t$]

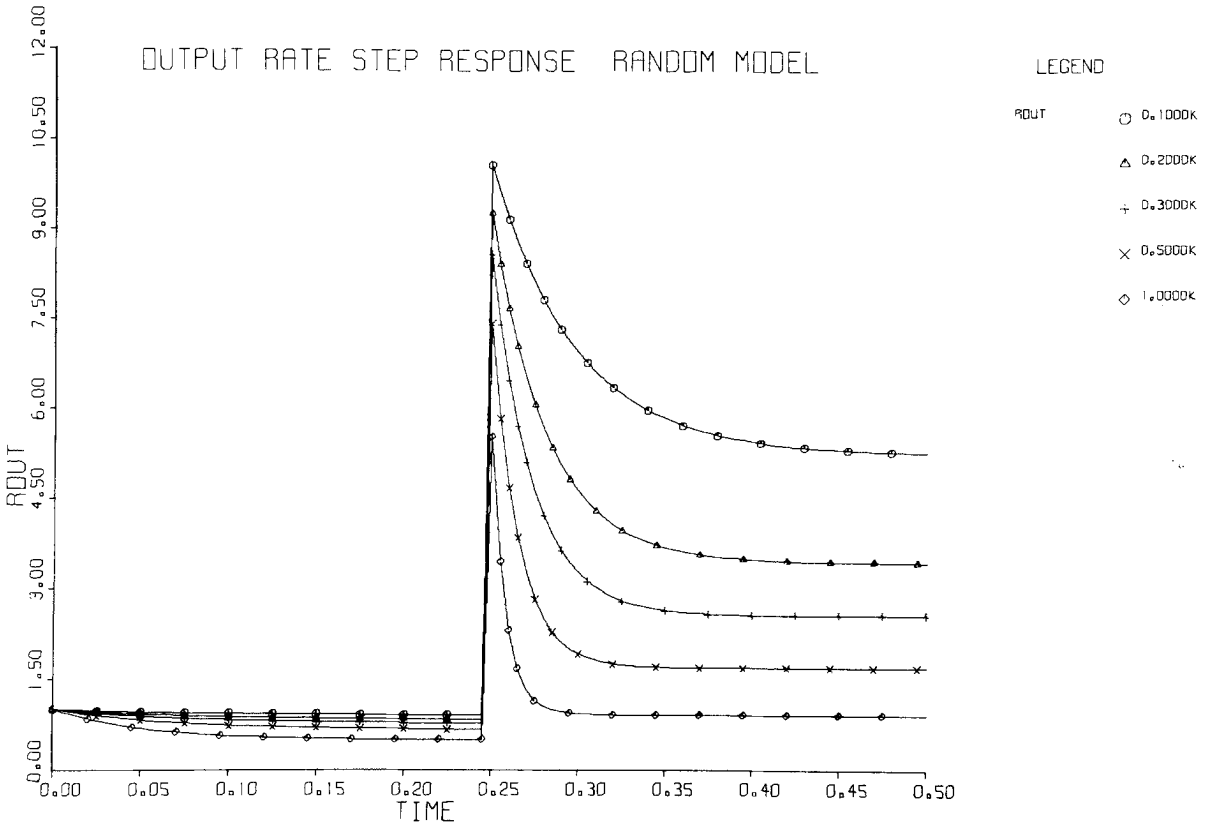

Fig. 8. Parametric set of random model (Fig. 5b) output rate step responses. Constant parameters are the feedback time constant $\tau = 0.1$, input amplitude $H = 10.0$, $\varrho_{x0} = 1.0$, and the running parameter is the feedback DC gain $K = 0.1, 0.2, 0.3, 0.5, 1.0$

reducing activity through a negative-feedback mechanism. Some effect of the input on other statistics (such as the standard deviation of the threshold random variable) could explain changes in firing regularity with input intensity. Temporal changes in output-dependent statistics of the threshold random variables are reflected in the local rate of jump points of the encoder quantizer as defined in Sect. IV. Thus $\varrho_x(x)$ at time t depends on the output rate $\varrho_{\text{out}}(t)$. We shall henceforth denote the implicit time dependence of the output controlled local quantizer jump point rate ϱ_x by $\varrho_x(t)$. Thus we can write the expression for the output rate of the random encoder, (10), for this case as:

$$\varrho_{\text{out}}(t) = \varrho_x(t) \cdot \lambda(t).$$

Defining the controlled jump point rate as:

$$\varrho_x(t) \triangleq \varrho_{x0} - \mathscr{H}[\varrho_{\text{out}}(t)]$$

where $\mathscr{H}$ denotes as before a general operator, we have

$$\varrho_{\text{out}}(t) = \{\varrho_{x0} - \mathscr{H}[\varrho_{\text{out}}(t)]\}\lambda(t). \tag{17}$$

Let us assume that $\mathscr{H}[\varrho_{\text{out}}(t)]$ has a positive d.c. gain of K. The arguments presented for the steady-state analysis in the deterministic case are still valid. Thus for a constant input λ_0 we have:

$$\varrho_{\text{out}_{ss}} = [\varrho_{x0} - K\varrho_{\text{out}_{ss}}]\lambda_0,$$

or

$$\varrho_{\text{out}_{ss}} = \frac{\varrho_{x0}\lambda_0}{1 + K\lambda_0}.$$

This expression for the steady-state firing rate indicates saturation at high input levels. Steady state responses to sinusoidal inputs can also be obtained analytically, assuming that the output becomes periodic and using its spectral decomposition.

A schematic diagram of the feedback model described above is presented in Fig. 5b. It is in fact a deterministic model accounting for random threshold effects in terms of the mean rates of firing only. Using a linear first-order low-pass filter for the feedback operator $\mathscr{H}$, one can write the system's equations similar to the deterministic case. Here, however, it is possible to obtain a closed form solution for step responses.

Given a feedback transfer function of $\mathscr{H}(s) = 1/(s\tau + 1)$, the output of which we denote by $\varrho_{x1}(t)$,

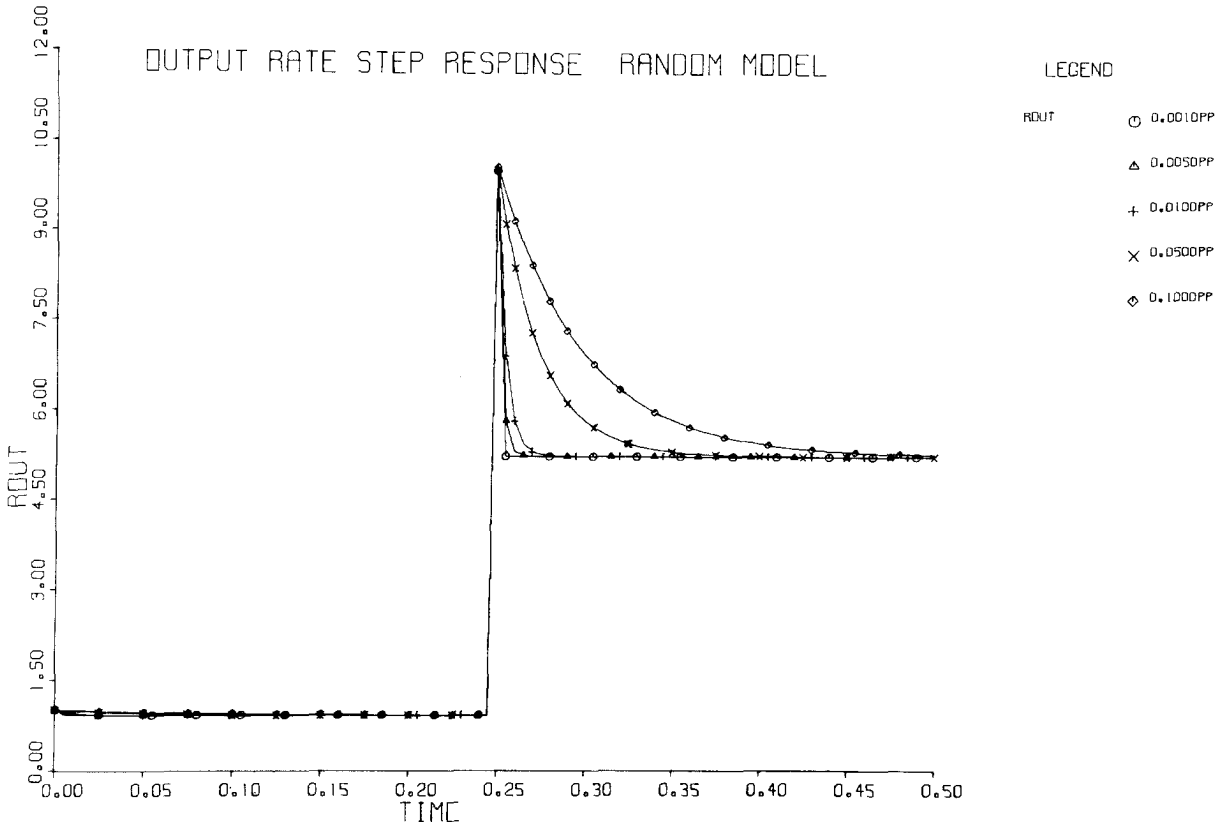

Fig. 9. Parametric set of random model (Fig. 5b) output rate step responses. The running parameter is the feedback time constant $\tau = 0.001$, 0.005, 0.01, 0.05, 0.1. Constant parameters are $K = 0.1$, $H = 10$, $\varrho_{x0} = 1.0$

the following equations for the adaptive system (Fig. 5b) are obtained:

$$\varrho_{\text{out}}(t) = \lambda(t)\,[\varrho_{x0} - K\varrho_{x1}(t)]$$

$$\tau \frac{d}{dt}\varrho_{x1}(t) + \varrho_{x1}(t) = \varrho_{\text{out}}(t),$$

yielding for $\varrho_{x1}(t)$ the differential equation with time-varying coefficients:

$$\frac{d}{dt}\varrho_{x1}(t) + \frac{1}{\tau}[1 + K\lambda(t)]\varrho_{x1}(t) = \frac{\varrho_{x0}}{\tau}\lambda(t).$$

For a step input $\lambda(t) = \lambda_0 u(t)$ and initial conditions due to constant background level of activity, represented in this model by the response to $\lambda(t) = 1$ for $t < 0$, the system equations provide the following expression for the response:

$$\varrho_{\text{out}}(t) = \varrho_{\text{out}_{ss}}\left[1 + \frac{K(\lambda_0 - 1)}{K+1} \cdot \exp(-t/\tau_s)\right], \tag{18}$$

with a steady state level $\varrho_{\text{out}_{ss}} = \dfrac{\varrho_{x0}\lambda_0}{1 + K\lambda_0}$ as obtained before, and an overall system time constant $\tau_s = \tau/(1 + K\lambda_0)$.

An interesting feature of the adaptive system is the dependence of the step response time constant on input amplitude and feedback gain. This is a well-known characteristic of adaptive gain control systems.

For a sinusoidal input the differential equation is rather difficult to integrate analytically; numerical methods which are possible are equivalent to the digital simulation of the system's behavior. The latter method was employed because of the convenience in using CSMP.

A parametric set of simulated step responses is presented in Figs. 8–10. Since we do not simulate a specific physiological system, and therefore do not seek specific parameter identifications, all variables in the simulations were normalized so that suitable scaling can be introduced. In Fig. 8, the varying parameter is the d.c. loop gain, K. This simulation demonstrates that the loop gain has an effect on both the level of the steady state and on the duration of the transient phase, in accordance with (18). The varying parameter in Fig. 9 is the time constant, τ, of the first-order low-pass feedback filter where, as expected, the shorter the time constant, the steeper the descent towards the steady state. As also expected, the input step amplitude has an

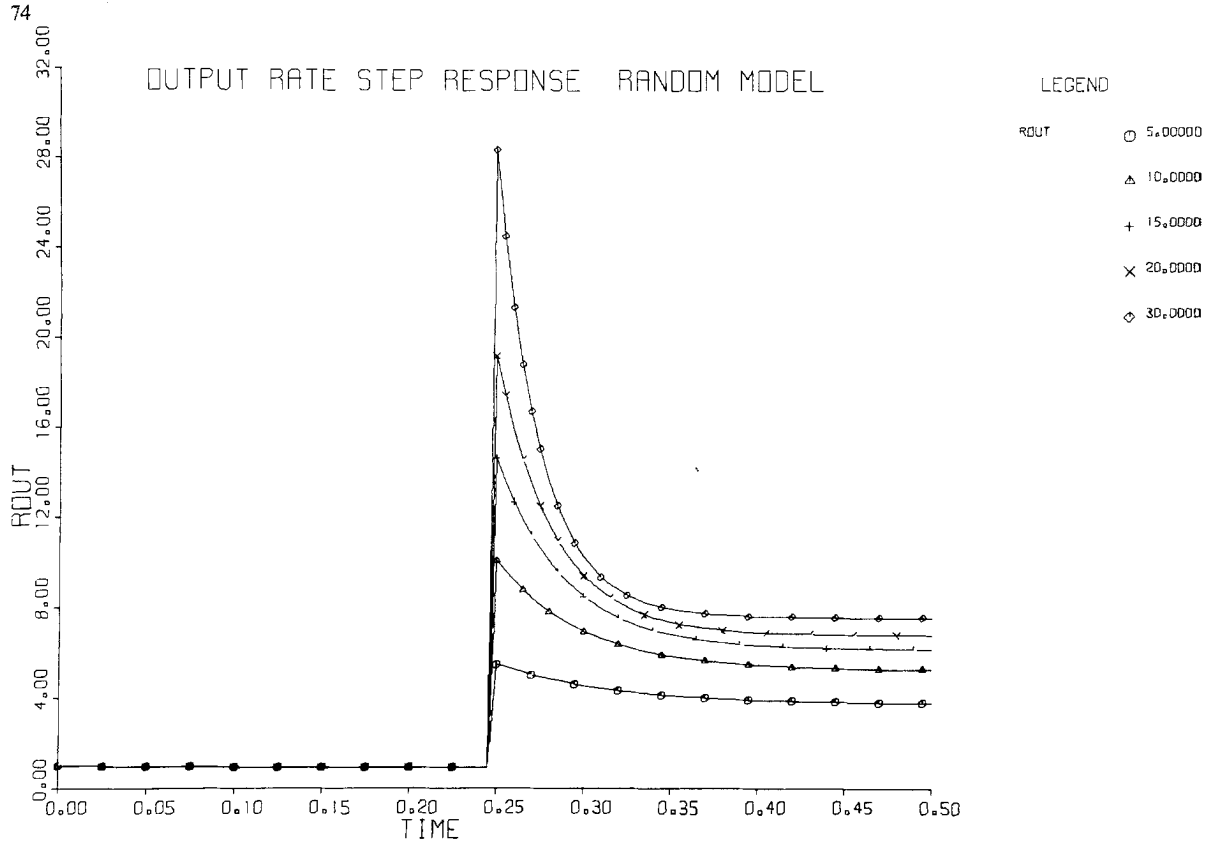

Fig. 10. Parametric set of random model (Fig. 5b) output rate step responses. The running parameter was $H=5$, 10, 15, 20, 30, constant parameters $K=0.1$, $\tau=0.1$, $\varrho_{x0}=1.0$

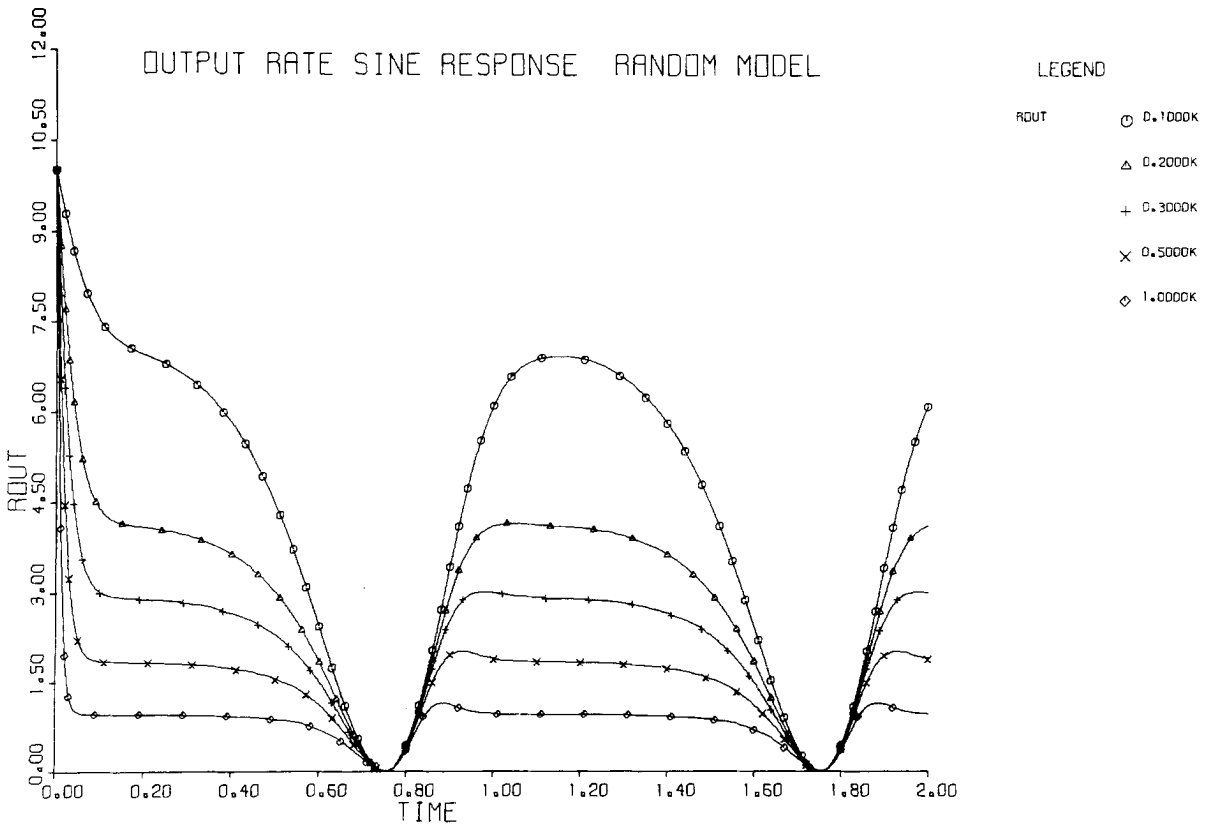

Fig. 11. Random model (Fig. 5b) sine responses. The running parameter was $K=0.1$, 0.2, 0.3, 0.5, 1.0 and constant parameters $\tau=0.1$, $\varrho_{x0}=1.0$, and $H=10$. [The input was $\lambda(t)=10+H\sin 2\pi t$, thus modulation depth $H/10=1$]

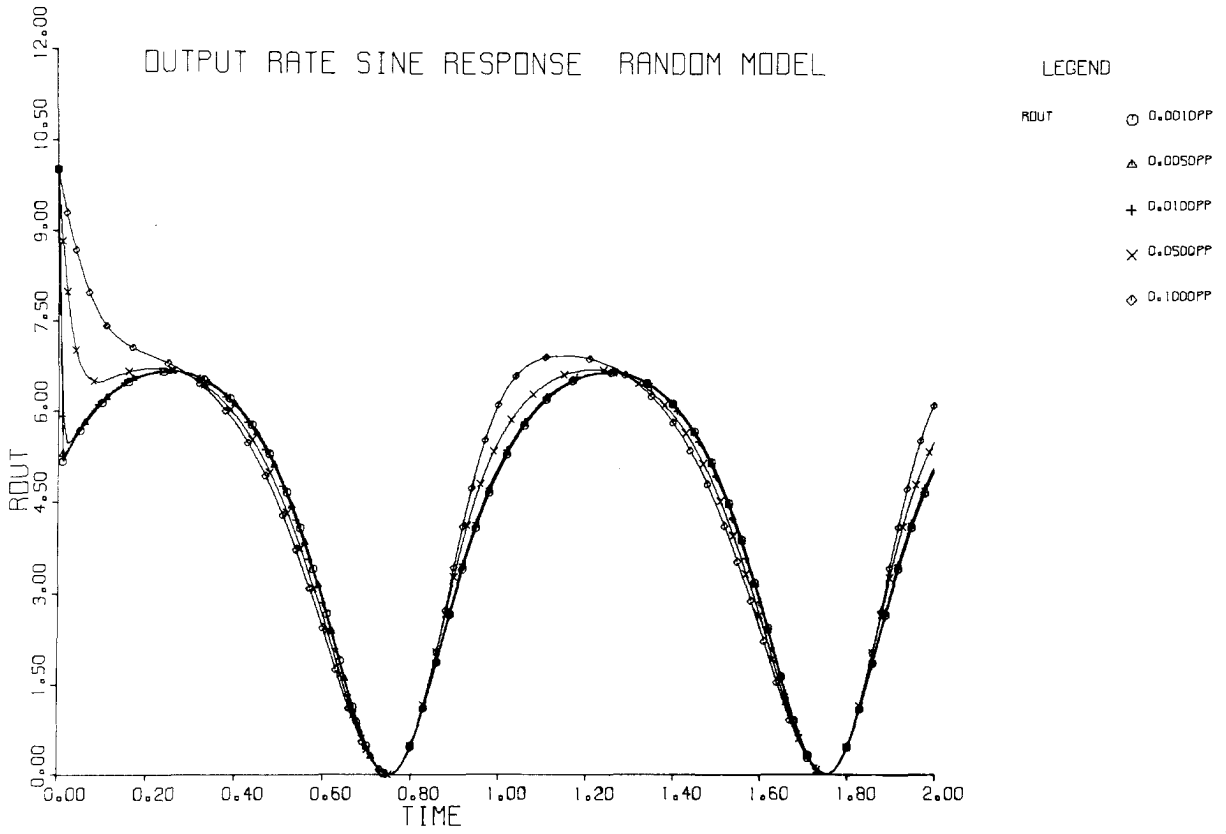

Fig. 12. Random model sine responses. The running parameter was $\tau = 0.001, 0.005, 0.01, 0.05, 0.1$, and constant parameters $K = 0.1$, $\varrho_{x0} = 1.0$, and $H = 10$. (Modulation depth 1)

effect both on the steady-state level finally reached and on the overall system's time constant (Fig. 10).

Simulated sine-wave responses are given in Fig. 11 through 13. For a given feedback time constant, increase of the loop gain results in drastic nonlinear suppression of the output's amplitude, hence in more pronounced distortions (Fig. 11). Given a relatively small loop gain, which yields a reasonable output dynamic range, the effect of reduced feedback time constants was reduction of total harmonic distortion (Fig. 12). Note that for longer time constants the resulting responses are quite asymmetric, with a higher rate of change of the output firing at the rising phase. The distortion became obviously weaker as the sinusoidal input amplitude decreased, with the attendant decrease in output modulation depth (Fig. 13). As noted in the simulation results, a saturation effect is recorded at high amplitudes of the input sinewave, its level being determined by the feedback gain, as shown in Fig. 11.

VI. Spectral Analysis

In this section, we discuss methods used in spectral analysis of deterministic and stochastic integrate-to-threshold models. A specific method for spectral analysis of SSIPFM, based on similarity to PPM as discussed in Sect. III (Zeevi and Bruckstein, 1977), is presented.

Spectral Analysis of SSIPFM *Signal*

Using the "functional encoder" defined by himself, Lee (1969) has shown that for the purpose of spectral analysis we can write an equivalent expression for $f_{\text{SSIPFM}}(t)$ as:

$$f_{\text{SSIPFM}}(t) = \lambda(t)\left[\frac{1}{A} + \frac{2}{A}\sum_{n=1}^{\infty}\cos\left\{\frac{2\pi n}{A}\int_0^t \lambda(\zeta)d\zeta\right\}\right]. \tag{19}$$

Lee's derivation of (19) proceeds as follows:

In the functional model (Fig. 2a), the quantizer is replaced by an equivalent parallel connection of a linear (L) and a nonlinear (NL) device (Fig. 14). The linear block, L, is defined as an amplifier with gain $1/A$, while the nonlinear, NL, device has a sawtooth input-output function. Thus (see Fig. 14)

$$\begin{aligned} y_1 &= \frac{1}{A}x \\ y_2 &= \frac{1}{A}(x - kA) \quad \text{for} \quad kA \leqq x < (k+1)A \end{aligned} \tag{20}$$

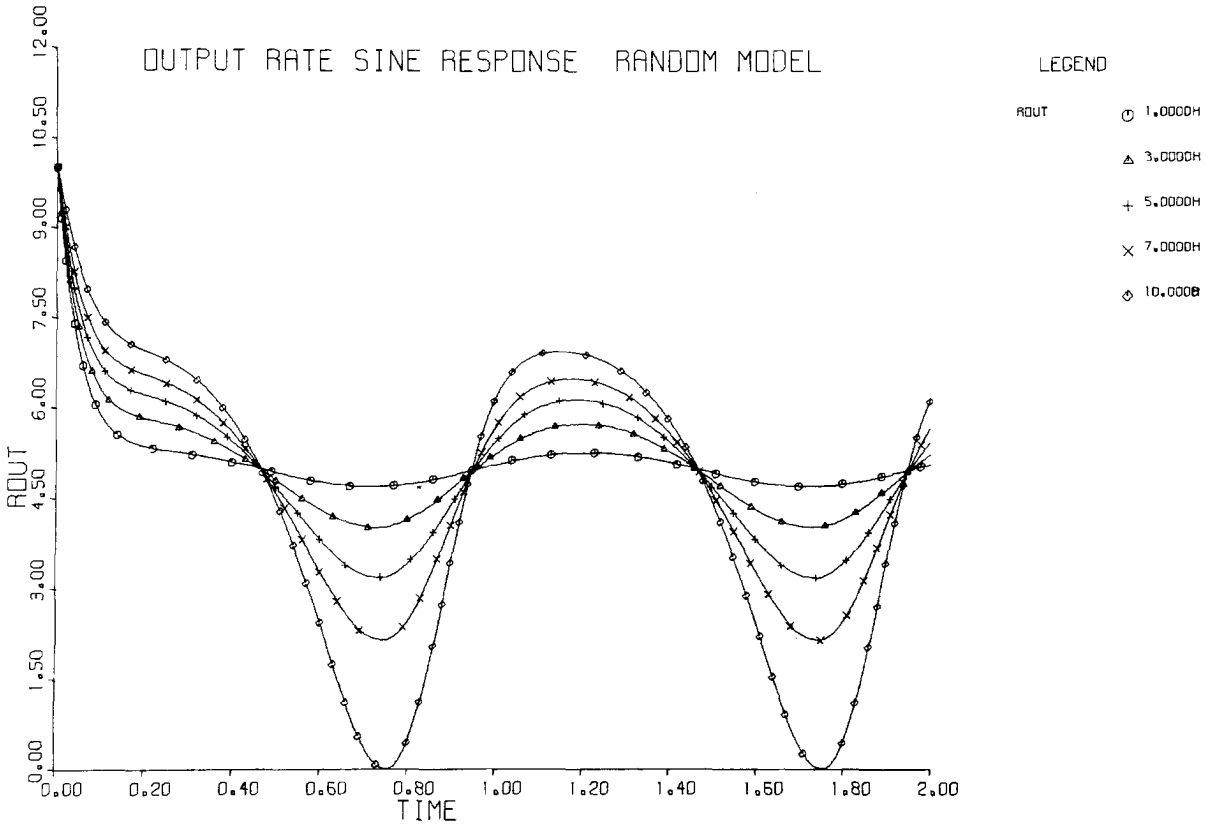

Fig. 13. Random model sine responses. The running parameter was $H=1, 3, 5, 7, 10$ (modulation depth of $H/10$) and constant parameters $K=0.1$, $\varrho_{x0}=1.0$, and $\tau=0.1$. The input was $\lambda(t)=10+H\sin 2\pi t$

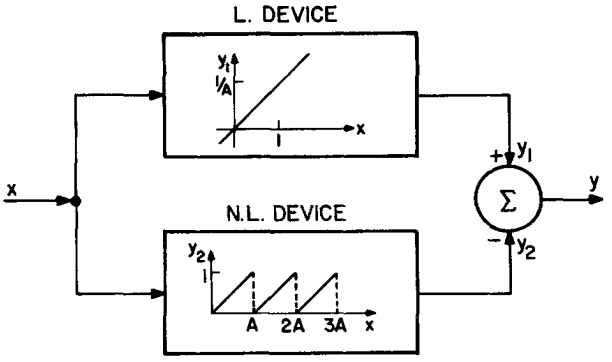

Fig. 14. Quantizer parallel-scheme equivalent (modified from Lee [19])

and thus the output of the parallel scheme is:

$$y=y_1(x)-y_2(x)=k \quad \text{for} \quad kA\leqq x<(k+1)A,$$

which is the quantizer transfer function.

Considering the functional model shown in Fig. 2a with the quantizer's equivalent, we have for the output:

$$f(t)=\frac{d}{dt}(y_1(x)-y_2(x))\,;$$

Substituting $\int_0^t \lambda(\zeta)d\zeta$ for x, we have

$$f(t)=\frac{d}{dt}\left[\frac{1}{A}\int_0^t \lambda(\zeta)d\zeta - y_2\left(\int_0^t \lambda(\zeta)d\zeta\right)\right],$$

which yields

$$f(t)=\lambda(t)\left[\frac{1}{A}-\frac{d}{dx}y_2(x)\bigg|_{x=\int_0^t \lambda(\zeta)d\zeta}\right]. \tag{21}$$

Writing the Fourier series for $y_2(x)$ and differentiating, we obtain:

$$\frac{dy_2(x)}{dx}=-\frac{2}{A}\sum_{n=1}^{\infty}\cos\frac{2\pi n}{A}x. \tag{22}$$

Again substituting $\int_0^t \lambda(\zeta)d\zeta$ for x in (22), and introducing this series into (21), we arrive at the expression given for the SSIPFM signal in (19).

We shall give here an analytical derivation of Eq. (19) based on the formalism devised by Rowe (1965) for analysis of the naturally sampled PPM Rowe's technique employs the following property of the Dirac delta function: if $g(t)$ is a function having a

single, simple zero at γ, [$g(\gamma)=0$ and $g(t)\neq 0$ iff $t\neq\gamma$], then:

$$\delta(t-\gamma)=\delta(g(t))|g'(t)|. \tag{23}$$

Let us define a function $g(t,k)$ as:

$$g(t,k)=\int_0^t \lambda(\zeta)d\zeta - kA. \tag{24}$$

It is readily verified that $g(t,k)$ is a monotonic increasing function of t, [$\lambda(t)>0$ by definition], $g(t,k)=0$ having the unique solution at $t=t_k$ [see Eq. (2)]. Furthermore, since $g'(t,k)=\lambda(t)$ is positive, we can write (23) for this case as:

$$\delta(t-t_k)=\delta(g(t,k))\lambda(t). \tag{25}$$

Substituting (25) for $\delta(t-t_k)$ in (2a), we have:

$$f_{\text{SSIPFM}}(t)=\lambda(t)\sum_k \delta(g(t,k))$$

or

$$f_{\text{SSIPFM}}(t)=\lambda(t)\sum_k \delta\left(\int_0^t \lambda(\zeta)d\zeta - kA\right). \tag{26}$$

We now define an auxiliary variable x as follows:

$$x\triangleq \int_0^t \lambda(\zeta)d\zeta. \tag{27}$$

Using Fourier expansion of a sequence of uniformly spaced (along the x-axis) delta functions (Papoulis, 1962), we formally obtain

$$\sum_{k=-\infty}^{+\infty}\delta(x-kA)=\frac{1}{A}+\frac{2}{A}\sum_{n=1}^{+\infty}\cos\frac{2\pi n}{A}x. \tag{28}$$

Now, substitution of (27) for x in (28) yields:

$$\sum_{k=-\infty}^{+\infty}\delta\left(\int_0^t \lambda(\zeta)d\zeta - kA\right)=\frac{1}{A}+\frac{2}{A}\sum_{n=1}^{\infty}\cos\left\{\frac{2\pi n}{A}\int_0^t\lambda(\zeta)d\zeta\right\}. \tag{29}$$

From (26) and (29) it follows immediately that:

$$f_{\text{SSIPFM}}(t)=\lambda(t)\left[\frac{1}{A}+\frac{2}{A}\sum_{n=1}^{\infty}\cos\left\{\frac{2\pi n}{A}\int_0^t\lambda(\zeta)d\zeta\right\}\right],$$

which is the required result stated in (19).

Thus, by applying the formalism of PPM spectral analysis to the SSIPFM signal, we readily arrive at the expression found by Lee. This fact also shows that there is intrinsic similarity between the PPM and SSIPFM (see results of Sect. III).

Note: Separating the input function, $\lambda(t)>0$, into its d.c. and a.c. components (as is usually done):

$$\lambda(t)=\lambda_{\text{dc}}+\lambda_{\text{ac}}(t),$$

and dividing $g(t,k)$ [defined in (24)] by λ_{dc}, we obtain:

$$\bar{g}(t,k)=t-k\frac{A}{\lambda_{\text{dc}}}+\frac{1}{\lambda_{\text{dc}}}\int_0^t\lambda_{\text{ac}}(\zeta)d\zeta.$$

Using $\bar{g}(t,k)$ instead of $g(t,k)$, we obtain the equivalent form for $f(t)$:

$$f_{\text{SSIPFM}}(t)=\left(1+\frac{1}{\lambda_{\text{dc}}}\lambda_{\text{ac}}(t)\right)\cdot\left[\sum_k\delta\left(t-k\frac{A}{\lambda_{\text{dc}}}+\frac{1}{\lambda_{\text{dc}}}\int_0^t\lambda_{\text{ac}}(\zeta)d\zeta\right)\right]. \tag{30}$$

The counterpart of this expression in the naturally sampled PPM, having a clock of period T and modulated by an input function $m(t)$, is (Rowe, 1965):

$$f_{\text{PPM}}(t)=(1-m'(t))\sum_k\delta(t-kT-m(t)), \tag{31}$$

where the derivative of the input, $m'(t)$, is less than 1. Now, comparing Eqs. (30) and (31), it is apparent that if

$$T=\frac{A}{\lambda_{\text{dc}}}\quad\text{and}\quad m(t)=-\frac{1}{\lambda_{\text{dc}}}\int_0^t\lambda_{\text{ac}}(\zeta)d\zeta,$$

we obtain $f_{\text{PPM}}(t)\equiv f_{\text{SSIPFM}}(t)$; these are also the results of Sect. III (5a, b).

Note that because $\lambda(t)>0$, we have

$$m'(t)=-\frac{\lambda_{\text{ac}}(t)}{\lambda_{\text{dc}}}<1,$$

which satisfies the requirement for PPM.

Equation (19) yields valuable insight into the spectral characteristics of the output $f(t)$. It is readily seen that the spectrum of the encoder output comprises that of the slowly changing input, $\lambda(t)$, as well as sidelobes centered at multiples of the frequency $2\pi\lambda_{\text{dc}}/A$, resulting from combined amplitude and frequency modulation.

Random Model Output Spectral Analysis

In Section IV, we presented a random integrate-to-threshold model which generates, subject to certain assumptions concerning the threshold random variables, a rate-modulated Poisson process. The nonuniform Poisson process is nonstationary and a specific technique is needed to obtain its spectral characteristics. Assuming that the modulating function, $\lambda(t)$, is a realization of a stationary and ergodic stochastic process, $\{A(t)\}$, we have the following result for the encoder output autocorrelation (Knox, 1970; Bartlett, 1963):

$$R_f(\tau)=\delta(\tau)\lambda_{\text{dc}}+R_A(\tau), \tag{32}$$

where $E[\lambda(t)] = \lambda_{dc}$ (ergodicity) and R_Λ is the autocorrelation of the process $\{\Lambda(t)\}$.

From (32) the spectrum is readily obtained as:

$$S_f(\omega) = \lambda_{dc} + S_\Lambda(\omega). \tag{33}$$

If $\{\Lambda(t)\}$ is a bandlimited process – or equivalently any realization $\lambda(t)$ is a slowly changing signal, – it is recoverable by low-pass filtering. The LPF output signal thus obtained is distorted by an additional flatspectrum component as indicated in (33), the signal-to-distortion ratio being

$$\frac{S}{D} = \frac{\int_{-W}^{+W} S_\Lambda(\omega) d\omega}{\lambda_{dc} 2W},$$

where W denotes the bandwidth of the LPF.

From the spectral analysis of the neural encoder output it is apparent that improvement in signal-to-distortion ratio is obtainable by signal amplification or, alternatively, by means of a multipath neural communication scheme (Knox, 1970; Bayly, 1968; Lee and Milsum, 1971; Milgram and Inbar, 1976).

VII. Discussion

Understanding of the functional characteristics of neural encoders is of paramount importance in analysis of neural communication systems. Because of the complexity of the processes involved, and in order to account for the vast volume of available experimental data, there is need for relatively simple models than can simulate the observed behavior qualitatively and thereby provide insight into the physiological mechanisms involved through mathematical analysis (Harmon and Lewis, 1966). As such, the integrate-to-threshold model has been previously employed both in analysis of neuronal encoders and sensory transducers (Gestri, 1971; Zeevi and Bruckstein, 1977; Stein et al., 1972; Knox, 1970; Stein and French, 1970), and as a component of complex neural information and control schemes (Lee and Milsum, 1971; Milgram and Inbar, 1976; Pavlidis, 1964).

Here, we were particularly interested in stochastic threshold fluctuations and adaptive phenomena. The latter were previously modeled using time-varying controlled membrane time constants and the leaky SSIPFM, with good fitting to experimental step-response data (Fohlmeister et al., 1974; Fohlmeister, 1973; Fohlmeister et al., 1977a, b). However, analysis of such models is quite complicated. In comparison the adaptive threshold control models, for both stochastic and deterministic cases, are relatively simple and straightforward, and yield good qualitative results in simulations. Furthermore, at least for some cases, closed form solutions indicating satisfactory adaptive properties are obtainable.

Both feedback and feedforward adaptive effects on threshold may be accomplished through voltage-dependent modulation of the concentration of molecules involved in opening or closing of ionic channels. Alternatively, such threshold control may be achieved through molecular conformational changes. However, in order to interpret the feedback or feedforward mechanism in molecular terms, we would have to confine the analysis to a specific receptor or neuron system, whereas the object of this paper is a general framework for modeling of adaptive threshold phenomena. This is also the rationale for normalization of system parameters and variables, so that suitable scaling can be readily introduced in any specific case.

Since changes in feedback gain affect the encoder's response time constants, the transfer characteristic of a population of cells may be modulated in concert through overall adaptive control of the cellular feedback gains. This may be mediated by lateral inhibition, by pooling of ionic channel blocking molecules, and/or by modulation of extracellular ionic concentrations. The behavior of overall adaptive populations of such cross-coupled encoder units is currently under investigation.

References

1. Bartlett, M.S.: The spectral analysis of point processes. J. R. Statist. Soc. B. Vol. **25**, 264–287 (1963)
2. Bayly, E.J.: Spectral analysis of pulse frequency modulation in the nervous system. IEEE Trans. Biomed. Eng. BME-**15**, 257–265 (1968)
3. Bullock, T.H.: Neuron doctrine and electrophysiology. Science **129**, 997–1002 (1959)
4. Carlson, A.B.: Communication systems. Tokyo: McGraw Hill Kogakusha 1975
5. Chung, S.-H., Raymond, S.A., Lettvin, J.Y.: Multiple meaning in single visual units. Brain Behav. Evol. **3**, 72–101 (1970)
6. Cole, K.S.: Ions and impulses – A chapter of classical biophysics. Berkeley: U.C. Berkeley Press 1968
7. Enroth-Cugell, C., Robson, J.G.: The contrast sensitivity of retinal ganglion cells of the cat. J. Physiol. **187**, 517–552 (1966)
8. Fohlmeister, J.F.: A model for phasic and tonic repetitively firing neuronal encoders. Kybernetik **13**, 104–112 (1973)
9. Fohlmeister, J.F., Poppele, R.E., Purple, R.L.: Repetitive firing: Dynamic behavior of sensory neurons reconciled with a quantitative model. J. Neurophysiol. **37**, 1213–1227 (1974)
10. Fohlmeister, J.F., Poppele, R.E., Purple, R.L.: Repetitive firing: A quantitative study of feedback in model encoders. J. Gen. Physiol. **69**, 815–848 (1977a)
11. Fohlmeister, J.F., Poppele, R.E., Purple, R.L.: Repetitive firing: Quantitative analysis of encoder behavior of slowly adapting stretch receptor of crayfish and eccentric cell of limulus. J. Gen. Physiol. **69**, 849–877 (1977b)
12. Friedman, B.: Principles and techniques of applied mathematics. New York: Wiley & Sons 1956

13. Gerstein, G.L., Perkel, D.H.: Mutual temporal relationships among neuronal spike trains. Biophys. J. **12**, 453–473 (1972)
14. Gestri, G.: Pulse frequency modulation in neural systems. Biophys. J. **11**, 98–109 (1971)
15. Harmon, L.D., Lewis, E.R.: Neural modelling. Physiol. Rev. **46**, 513–591 (1966)
16. Hodgkin, L.: The conduction of nervous impulse. Springfield, Ill.: Thomas 1964
17. IBM System/360 Continuous System Modelling Program – System Manual
18. Knox, C.K.: Signal transmission in random spike trains with applications to the statocyst neurons of the lobster. Kybernetik **7**, 167–174 (1970)
19. Lee, H.C.: Integral pulse frequency modulation with technological and biological applications. Ph.D. dissertation, McGill Univ., Montreal, Quebec, 1969
20. Lee, H.C., Milsum, J.H.: Statistical analysis of multiunit, multipath neural communication. Math. Biosci. **11**, 181–202 (1971)
21. Li, C.C.: Integral pulse frequency modulated control systems. Ph.D. dissertation, Northwestern University, Illinois, 1961
22. Milgram, P., Inbar, G.F.: Distortion suppression in neuromuscular information transmission due to interchannel dispersion in muscle spindle firing thresholds. IEEE Trans. Biomed. Eng. BME-**23**, 1–15 (1976)
23. Papoulis, A.: Probability, Random variables, and stochastic processes. New York: McGraw Hill 1965
24. Papoulis, A.: The Fourier integral and its applications. New York: McGraw Hill 1962
25. Pavlidis, T.: Analysis and synthesis of pulse frequency modulation feedback systems. Ph.D. dissertation, University of California, Berkeley, 1964
26. Perkel, D.H., Bullock, T.M.: Neural coding. Neurosci. Res. Program Bull. **6**, 221–348 (1968)
27. Perkel, D.H.: Spike trains as carriers of information. In: The neurosciences, second study program. Schmidt, F.O. (ed.), p. 587. New York: Rockefeller Univ. 1970
28. Poppele, R.E., Chen, W.J.: Repetitive behavior of mammalian muscle spindle. J. Neurophysiol. **35**, 357–364 (1972)
29. Rowe, H.E.: Signals and noise in communication systems. New Jersey: Van Nostrand Comp. 1965
30. Sanderson, A.C., Calvert, T.W.: Distribution coding in neural interaction models. Internal Report, Carnegie-Mellon University, Pittsburgh, PA, 1973
31. Segundo, J.P.: Communication and coding by nerve cells. In: The neurosciences, second study program. Schmidt, F.O. (ed.), p. 569. New York: Rockefeller Univ. 1970
32. Siebert, W.M.: Frequency discrimination in the auditory system: Place of periodicity mechanism? Proc. IEEE **58**, 723–730 (1970)
33. Snyder, D.L.: Random point processes. New York: Wiley & Sons 1975
34. Stein, R.B.: The role of spike trains in transmitting and distorting sensory signals. In: The neurosciences, second study program. Schmidt, F.O. (ed.), p. 597. New York: Rockefeller Univ. 1970
35. Stein, R.B., French, A.S., Holden, A.V.: The frequency response, coherence, and information capacity of two neuronal models. Biophys. J. **12**, 295–322 (1972)
36. Stein, R.B., French, A.S.: Models for the transmission of information by nerve cells. In: Proc. Fifth International Meeting of Neurophysiologists, Oslo, 1970
37. Sugiyama, H., Moore, G.P., Perkel, D.H.: Solutions for a stochastic model of neuronal spike production. Math. Biosci. **8**, 323–341 (1970)
38. Terzuolo, C.A.: Data transmission by spike trains. In: The neurosciences, second study program. Schmidt, F.O. (ed.), p. 661. New York: Rockefeller Univ. 1970
39. Verveen, A.A., De Felice, L.J.: Membrane noise. Prog. Biophys. Mol. Biol. **28**, 189–265 (1974)
40. Verveen, A.A., Derksen, H.E.: Fluctuation phenomena in nerve membrane. Proc. IEEE **56**, 906–915 (1968)
41. Walløe, L.: Transfer of signals through a second order sensory neuron. Inst. of Physiology, Univ. Oslo, 1968
42. Wright, M.J., Ikeda, H.: Processing of spatial and temporal information in the visual system. In: The neurosciences, third study program. Schmidt, F.O., Worden, F.G. (eds.). Cambridge, MA: MIT Press 1974
43. Zeevi, Y.Y., Bruckstein, A.M.: A note on single signed integral pulse frequency modulation. IEEE Trans. Syst. Man Cybern. **SMC-7**, 875–877 (1977)

Received: January 11, 1979

Prof. Dr. Y. Y. Zeevi
Department of Electrical Engineering
Technion-Israel Institute of Technology
Technion City
Haifa 32000, Israel